

Tuning a sign of magnetoelectric coupling in paramagnetic $\text{NH}_2(\text{CH}_3)_2\text{Al}_{1-x}\text{Cr}_x(\text{SO}_4)_2 \times 6\text{H}_2\text{O}$ crystals by metal ion substitution

Published online: 26 October 2017

V. Kapustianyk^{1,2}, Yu. Eliyashevskyy², Z. Czaplak^{3,4}, V. Rudyk¹, R. Serkiz¹, N. Ostapenko², I. Hirnyk¹, J.-F. Dayen⁵, M. Bobnar⁶, R. Gumeniuk⁷ & B. Kundys^{5,*}

Hybrid organometallic systems offer a wide range of functionalities, including magnetoelectric (ME) interactions. However, the ability to design on-demand ME coupling remains challenging despite a variety of host-guest configurations and ME phases coexistence possibilities. Here, we report the effect of metal-ion substitution on the magnetic and electric properties in the paramagnetic ferroelectric $\text{NH}_2(\text{CH}_3)_2\text{Al}_{1-x}\text{Cr}_x(\text{SO}_4)_2 \times 6\text{H}_2\text{O}$. Doing so we are able to induce and even tune a sign of the ME interactions, in the paramagnetic ferroelectric (FE) state. Both studied samples with $x = 0.065$ and $x = 0.2$ become paramagnetic, contrary to the initial diamagnetic compound. Due to the isomorphous substitution with Cr the ferroelectric phase transition temperature (T_c) increases nonlinearly, with the shift being larger for the 6.5% of Cr. A magnetic field applied along the polar c axis increases ferroelectricity for the $x = 0.065$ sample and shifts T_c to higher values, while inverse effects are observed for $x = 0.2$. The ME coupling coefficient $\alpha_{\text{ME}} = 1.7 \text{ ns/m}$ found for a crystal with Cr content of $x = 0.2$ is among the highest reported up to now. The observed sign change of α_{ME} with a small change in Cr content paves the way for ME coupling engineering.

Realization of the electric interactions between magnetic moments and electric charges constitutes an important task for modern solid state physics^{1,2} and spin electronics^{3,6}. The principal motivation is to establish electric control of magnetism for low-power spintronic structures. For this reason large scales of magnetization and electric polarization are often motivating factors for multiferroic materials research^{7,9}. Although large magnetization is expected from ferromagnetic ordering, ferromagnetism and ferroelectricity tend to be mutually exclusive in a single phase¹⁰ and the largest magnetoelectric coupling is mostly seen in antiferromagnets at symmetry-breaking spin reorientation transitions¹¹. However, ME coupling of higher orders can be symmetry independent and exists for other types of magnetic orderings^{12,13}. In particular, a large ME effect, as reported to exist in the paramagnetic $[(\text{CH}_3)_2\text{NH}_2]\text{Mn}(\text{HCOO})_3$ ¹⁴. Along with other successful examples^{15,20}, this result demonstrates a large potential of organic-inorganic materials²¹ in the research of ME compounds and beyond^{22,23}. Because electric order in the lattice is more fragile than a magnetic one, a promising strategy to achieve their safe coexistence can be implementation of magnetic interactions into already known electrically polar compounds rather than vice versa. In this respect the organic-inorganic hybrid frameworks offer indeed an abundance of possibilities²⁴⁻³². Here we study the ferroelectric $\text{NH}_2(\text{CH}_3)_2\text{Al}(\text{SO}_4)_2 \times 6\text{H}_2\text{O}$ (DMAAS) crystals which belong to organic-inorganic functional materials known to be electrically polar below 152 K^{33,34}. The crystal structure of DMAAS is built up of Al cations coordinated by six water molecules (i.e. water octahedra), regular $(\text{SO}_4)^{2-}$ tetrahedra and $[\text{NH}_2(\text{CH}_3)_2]^+$ (DMA) cations, all hydrogen bonded to a three dimensional framework (Fig. 1).

¹Scientific-Technical and Educational Center of Low-Temperature Studies, Ivan Franko National University of Lviv, Dragomanova str. 50, 79005, Lviv, Ukraine. ²Department of Physics, Ivan Franko National University of Lviv, Dragomanova str. 50, 79005, Lviv, Ukraine. ³Department of Physics, Opole University of Technology, Ozimska 75, 45370, Opole, Poland.

⁴Institute of Experimental Physics, University of Wrocław, pl. M. Borna 9, 50204, Wrocław, Poland. ⁵Institute de Physique et de Chimie des Matériaux de Strasbourg, UMR 7504 CNRS-ULP, 23 rue du Loess, BP 43, F67034, Strasbourg, Cedex 2, France. ⁶Max Planck Institut für Chemische Physik fester Stoffe, Nöthnitzer Str. 40, 01187, Dresden, Germany. ⁷Institut für Experimentelle Physik, TU Bergakademie Freiberg, Leipziger Str. 23, 09596, Freiberg, Germany. Correspondence and requests for materials should be addressed to B.K. (+email: kundys@tipcms.unistra.fr)

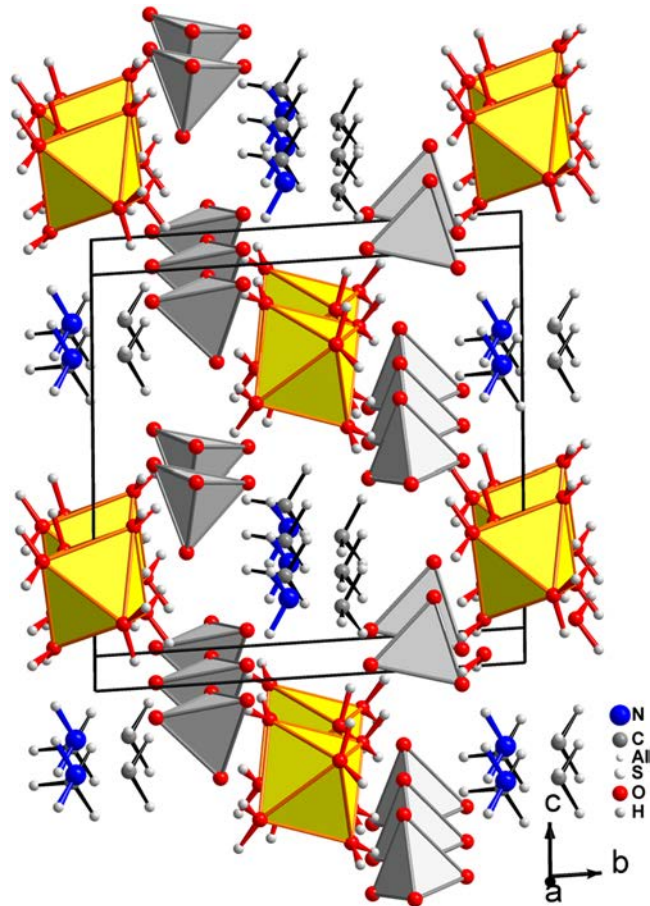


Figure 1. Crystal structure of non-centrosymmetric monoclinic $[\text{NH}_2(\text{CH}_3)_2]\text{Al}(\text{SO}_4)_2 \times 6\text{H}_2\text{O}$ at 135 K. The Al atoms are in the centers of yellow $[\text{H}_2\text{O}]_6$ -octahedra. In the case of Cr substitution the octahedra are occupied by statistical mixtures of magnetic Cr and nonmagnetic Al atoms. The $[\text{SO}_4]^{2-}$ tetrahedra are depicted in grey color.

in the crystal structures of $[\text{NH}_2(\text{CH}_3)_2]\text{Al}_{1-x}\text{Cr}_x(\text{SO}_4)_2 \times 6\text{H}_2\text{O}$ with $x=0.2$ and 0.065 octahedra are occupied by statistical mixtures of magnetic Cr^{3+} and nonmagnetic Al^{3+} atoms. With cooling this crystal exhibits a second order phase transition at $T_c=152\text{ K}$ from paraelectric to ferroelastic ($T > T_c$) to ferroelectric ($T < T_c$) phases. The phase transition is of the order-disorder type with a symmetry change $2/m \rightarrow m$. It is connected with ordering of the polar DMA cations which exhibit hindered rotations around their C-C direction in the paraelectric phase and order only in the spatio-temporal average in the ferroelectric phase³⁵. Metal ion isomorphous substitution in the above mentioned family of compounds can be an additional degree of freedom in the composition-property engineering^{36,37}. Here we report that the incorporated magnetic Cr cations can participate in ME interactions in the $[\text{NH}_2(\text{CH}_3)_2]\text{Al}_{1-x}\text{Cr}_x(\text{SO}_4)_2 \times 6\text{H}_2\text{O}$ crystals with ability to tune magneto-electric functionality.

Results

Initial DMAAS crystals grow in a monodomain ferroelastic state. The ferroelastic domains may nevertheless appear during polishing or other type of mechanical treating. However, if Cr is introduced this tendency is reversed: the samples predominantly grow in a pol domain ferroelastic state (Fig. 2). In this case the EDX analysis of the neighboring domains shows a different content of chromium. The equal ratio of Cr in oppositely stressed domains is equal to 17.6% and 20% respectively. In principle, however, it does not apply to minor quantities of samples that grow in the single domain state where chromium is distributed evenly within a sample. It is observed that thermodynamic conditions of the growth are highly stress-dependent and allow variation of the Cr distribution within the sample. This is an intriguing result, however, deserves separate investigations that are beyond the scope of this paper. During our further discussion we will consider only the crystals grown in a pol domain states as this type of growth is statistically easier to handle. The average thickness of domains was found to be equal to $100\text{ }\mu\text{m}$, with the optical indicatrix disorientation angle of $2\theta=40^\circ$.

The existence of a pol domain ferroelastic state was also verified by scanning electron microscopy imaging (Fig. 2c,d). Similarly to the initial composition of samples shows large peaks in the dielectric permittivity due to the polar state formation at $T_c=153\text{ K}$, which is characteristic for proper ferroelectric phase transitions (Fig. 3). Notably, the value of the dielectric permittivity is almost three orders of magnitude larger for an AC electric field applied along the c axis concerning the spontaneous polarization direction (Fig. 3a). The temperature

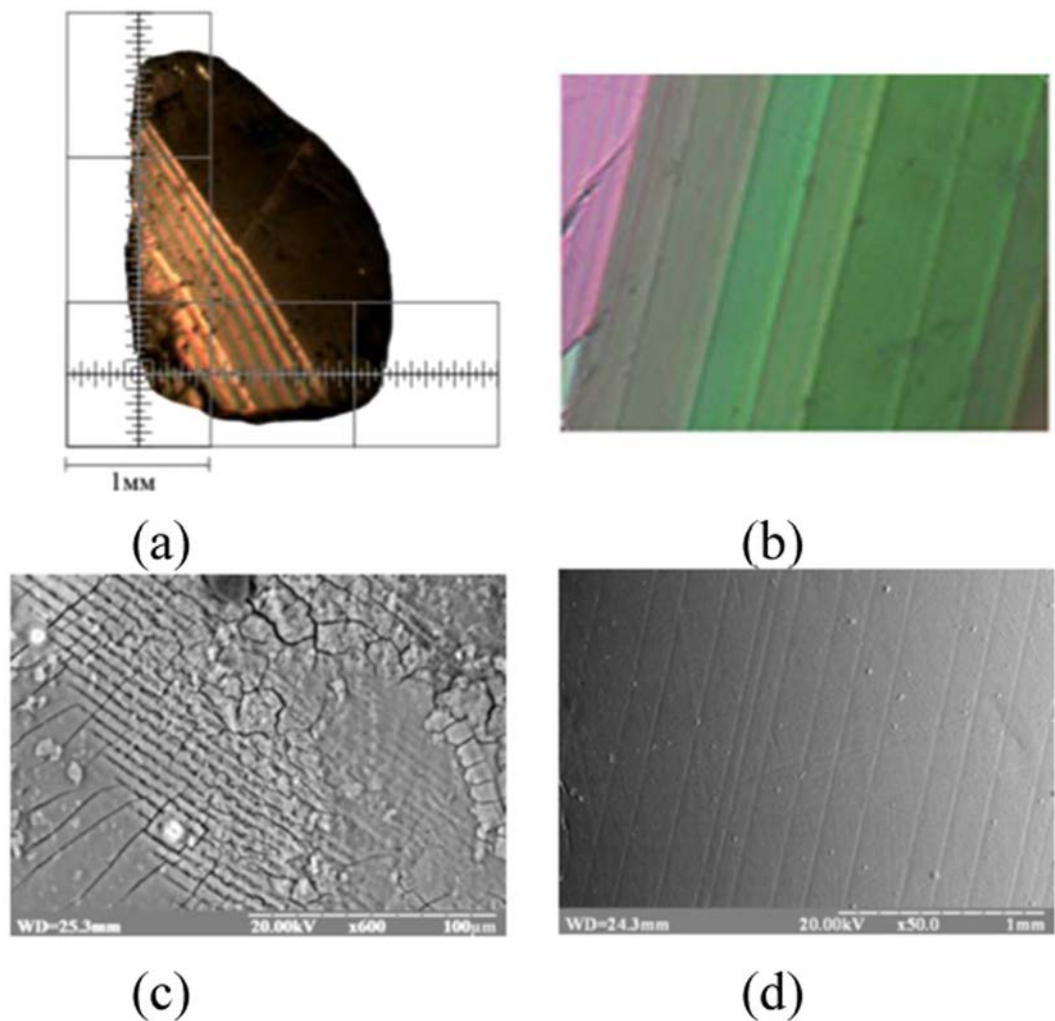


Figure 2. Ferroelastic domain structures at 300 K. Polarization micrograph pictures on the c face of DMAAl_{0.8}Cr_{0.2}S crystals perpendicular to [310] (a,b) and corresponding Δd_{ν} of the (001) (c) and (310) (d) surfaces of the same crystals obtained using a scanning electron microscope in TOPO and TOPO regimes respectively.

dependences of the thermal expansion measured along the three principal axes of a DMAAl_{0.8}Cr_{0.2}S crystal are presented in Fig. 3b. The clear continuous changes of all three lattice parameters are characteristic of a second order phase transition and confirm its structural component. The piezoelectric measurements for DMAAl_{0.8}Cr_{0.2}S confirm and complement the electrically polar character of the transition.

A distinct clear peak in the current is observed at the same temperature where both dielectric permittivity and thermal expansion also show anomalies. A DC electric field of 7.9 kV/m applied during cooling reveals peaks in the piezoelectric currents for both samples and demonstrates Cr dependent T_c evolution. The temperature dependences of the dielectric properties for both investigated crystals fairly well correlate with the data of previous investigations³⁷ and obey the Curie-Weiss law both in the paraelectric (+) and ferroelectric (-) phases in the vicinity of the ferroelectric phase transition. Together with the data of DSC studies³⁷ this clearly confirms a second order of the phase transition. No other anomalies were observed in the piezoelectric temperature dependences of both samples down to 1.6 K. Therefore, one can conclude that the ferroelectric phase exists in our DMAAl_{1-x}Cr_xS crystals in the temperature range from T_c down to 1.6 K. This conclusion is also confirmed by the temperature dependences of the electric polarization (Fig. 4a) measured at a ferroelectric saturation occurring above 250 kV/m³⁸. The magnetic susceptibilities of DMAAl_{1-x}Cr_xS complexes are depicted in the inset to Fig. 4b along with electric polarization data (Fig. 4a). The piezoelectricity of Cr (x=0) is diamagnetic in the whole studied temperature range with residual susceptibility χ_0 given in Table 1.

Isomorphous substitution of Al with Cr leads to the appearance of a paramagnetic fraction below 100 K for $x=0.06$ and to a paramagnetic behavior and, thus positive $\chi(T)$ for $x=0.2$ (inset to Fig. 4b). Both these susceptibilities are essentially modified Curie-Weiss (CW) law ($\chi = C/T + \chi_0$) in the temperature range 50–300 K (inset to Fig. 4b). As one can see from Table 1 the χ_0 values obtained from the fit agree well with those of initial DMAAS crystals. This confirms that Cr-atoms are embedded into a diamagnetic matrix. Electric magnetic

... Cr states and temperature independent susceptibility derivative for the crystal ... $x=0.2$ an optimum occurs towards high temperature. ... correlates well with the different magnetic ... ferroelectric correlation temperature position for both samples (Fig. ... magnetic field the peak in piezoelectric increases and shifts towards ... promotes ferroelectricity) ... compound with $x=0.065$, while for $x=0.2$ the only ... (Fig. 5). The ME coupling coefficient α_{ME} in the units of [s/m] is defined here as

$$\alpha_{ME} = \frac{1}{I} \left(\frac{dP}{dH} \right) dt$$

where I is the piezoelectric coefficient and H is the magnetic field applied ($H\mu_0 = 6$ T) during the measurements (Fig. 5). As one can see from the coupling coefficient presented in Fig. 6, the effect of coupling is stronger for the crystal with $x=0.2$. As expected, the ... ferroelectricity.

However, the ... shows a discontinuity in ME coupling near T_c (inset to Fig. 6) implying the existence of a ... in the paraelectric and paramagnetic region. The fact that the ME coupling coefficient ... as a function of Cr content as well as the large level of the coupling itself points towards the ... the ME response in such compounds.

The ME properties can be tentatively explained by the twofold effect. Firstly, the introduction of larger $r_{Cr} = 0.6115$; $r_{AL} = 0.535$)⁶⁹ and magnetic Cr generates strains and secondly, makes the compound more sensitive to magnetic field. The magnetoelectric coupling here can arise via stress mediated contribution. With content increase the overall sample deformation goes via critical point modifying local magnetism and polarization. This assumption seems to be in agreement with the sensitive ferroelastic structure. This issue, however, requires a separate study including optimal Cr content determination.

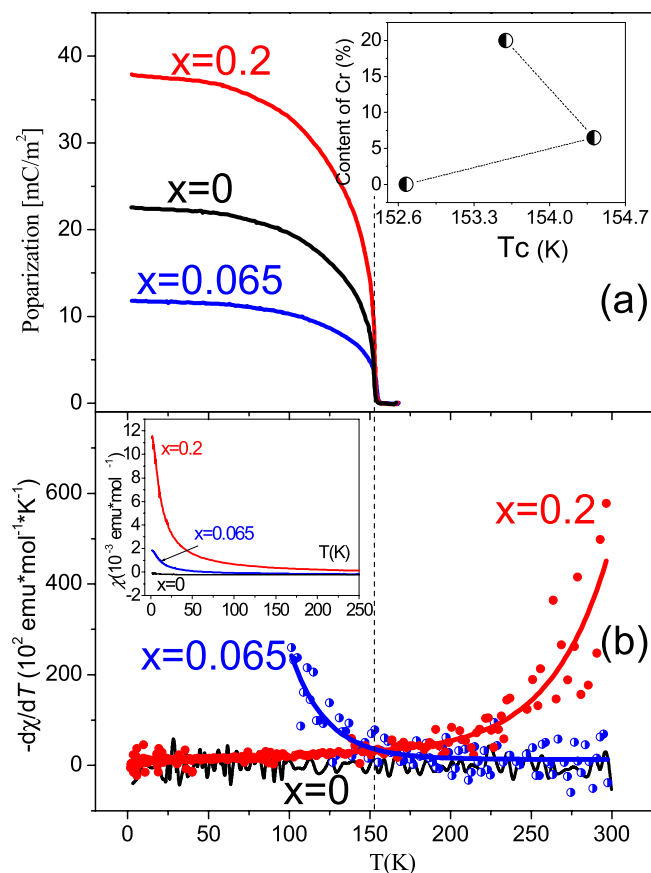


Figure 4. Temperature dependence of magnetic and electric properties. (a) Electric polarization. (b) Derivatives of susceptibilities for DMAAAl_{1-x}Cr_xS crystals with different Cr content. Insets in (a) and (b) show, respectively, a variation of the ferroelectric transition temperature T_c and magnetic susceptibilities from which magnetic parameters are determined via CW (Table 1).

Cr-content, x	χ_0 (10^{-4} emu mol ⁻¹)	μ_{eff} (μ_B)
0	-2.26(7)	
0.06	-2.40(5)	1.47(1)
0.2	-2.49(8)	1.91(1)

Table 1. Magnetic parameters for DMAAAl_{1-x}Cr_xS crystals.

In conclusion, this study reports the successful creation of paramagnetic order in the initial diamagnetic DMAAS crystal isomorphous substitution of metal ion. Such action intimately connects apparently separated magnetic and electric subsystems, as evidenced by the temperature dependence of the derivative magnetic susceptibility. We have successfully generated a large ME coupling and importantly demonstrated the possibility to tune its sign, depending on the Cr content. Moreover, our results suggest that ME coupling can exist in the paramagnetic compounds with the easily noticeable magnetic anomalies near FE transitions, and special care should be taken for such evidence. From the ferroelectric point of view, we show that partial isomorphous substitution with Cr metal ions leads to an noticeable shift of the phase transition and can be used to increase FE polarization and T_c . In particular, in comparison with initial DMAAS crystal, the phase transition temperature T_c in the crystal doped with Cr³⁺ (6.5%) is shifted to a higher temperature by 2.6 K, whereas for a higher chromium concentration (20%), this shift is diminished to 0.6 K. The Cr distribution in such samples can also be controlled by stress-assisted material growth conditions and provides additional degrees of freedom for organometallic materials engineering. Our study motivates further investigations in the area of paramagnetic organic-inorganic materials, with the design of ME interactions at room temperature as the next milestone.

Methods

Single crystals of [NH₂(CH₃)₂]Al_{1-x}Cr_x(SO₄)₂ × 6H₂O (DMAAAl_{1-x}Cr_xS) were grown from an aqueous solution containing the metal sulphates in a stoichiometric ratio and dimethylammonium salt at a constant temperature of 303 K by slow evaporation method. The molar ratio of Al³⁺:Cr³⁺ in the solution was equal to 1:0.065 and

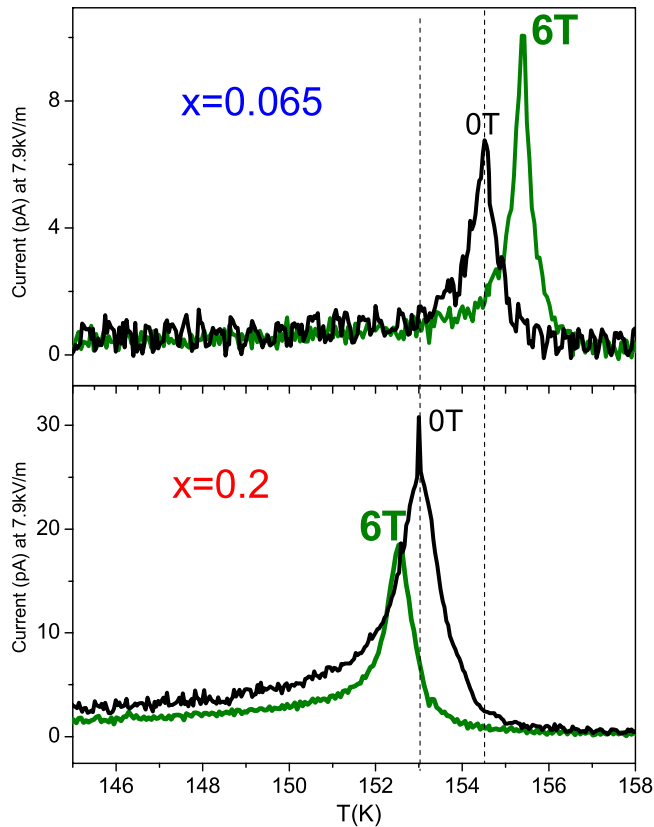


Figure 5. Magnetic field influence on the piezoelectricity. Upper panel: the sample with the Cr content of $x=0.065$; Lower panel: the sample with the Cr content of $x=0.2$. An opposite behavior in both magnitude and temperature position of the piezoelectric peak is observed.

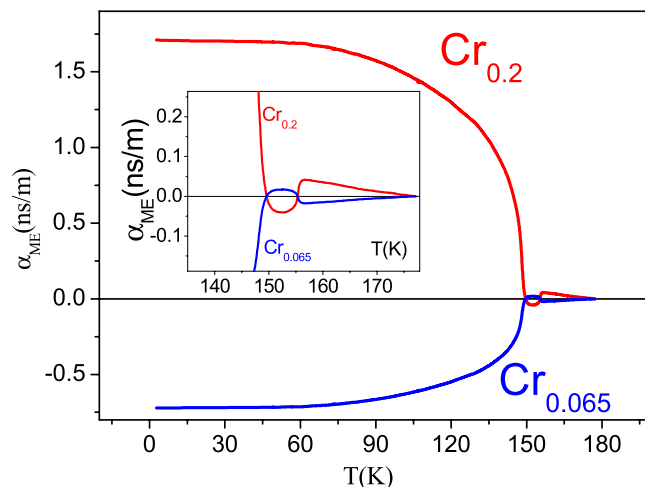


Figure 6. Temperature dependence of the ME coupling coefficients for parallel orientation of magnetic and electric fields. Inset shows a zoomed region near T_c .

1:0.2, respectively, is ratio in the samples as controlled by SEM using a REA A-102 02 (SEMI, Ukraine) scanning electron microscope. Quantitative electron probe microanalysis (EPMA) of the phases was carried out using an energy-dispersive X-ray (EDX) analyzer with the pre-elements as standards (the acceleration voltage was 20 kV; K- and L-lines were used). The obtained values of Al^{3+} : Cr^{3+} molar ratio were found to be 0.065 ± 0.006 and 0.2 ± 0.02 (for a single domain samples) and correspond to those in the reacting solution. The surface morphology was studied by SEM. The scanning of samples surface was performed by an electron beam with energy of 15 and 20 kV and a diameter of 5 nm in the secondary electron image regime. To prevent charging during SEM cycling, the sample was coated by a thin graphite layer transparent for the electron beam. The thermal expansion

as measured using a home-built capacitance dilatometer. The measurements of the real part of dielectric permittivity and conductivity were carried out using the traditional method of capacitor capacitance measurement. The capacitance was measured using an automated setup based on a LCR-meter HIOKI 3522-50 LCF HiTester. The spontaneous polarization was measured using Keithley 6517 A electrometer. The magnetic susceptibility was measured using a commercial magnetometer Quantum Design MPMS-3 in the temperature range 1.8–300 K and magnetic fields up to $\mu_0 H = 7$ T. For both polarization and magnetic measurements electric and magnetic fields were applied perpendicular to the crystallographic plane in the monoclinic crystal structure (parallel to the polar axis).

References

1. Fiebig, M. Review of the magnetoelectric effect. *J. Phys. Appl. Phys.* **38**, 123 (2005).
2. Cheong, S.-W. & Mostoio, M. M. Multiferroics: a magnetic vector for ferroelectricity. *Nat. Mater.* **6**, 13–20 (2007).
3. Bibes, M. & Barthélémy, A. M. Multiferroics: Towards a magnetoelectric memory. *Nat. Mater.* **7**, 425–426 (2008).
4. Binck, C. & Dodin, B. Magneto-electronics with magneto-electrics. *J. Phys. Condens. Matter* **17**, L39 (2005).
5. Bogani, L. & Wernsdorfer, W. Molecular spintronics using single-molecule magnets. *Nat. Mater.* **7**, 179–186 (2008).
6. Cinchetti, M., Dedi, V. A. & Hesse, L. E. Activating the molecular spin interface. *Nat. Mater.* **16**, 507–515 (2017).
7. Di Sante, D., Stroppa, A., Jain, P. & Picozzi, S. Tuning the ferroelectric polarization in a multiferroic metal-organic framework. *J. Am. Chem. Soc.* **135**, 18126–18130 (2013).
8. Kundys, B. *et al.* Multiferroicity and hydrogen-bond ordering in $(C_2H_5NH_3)_2C_2Cl_4$ featuring dominant ferromagnetic interactions. *Phys. Rev. B* **81**, 224434 (2010).
9. Huang, B. *et al.* Importing spontaneous polarization into a Heisenberg ferromagnet for a potential single-phase multiferroic. *J. Mater. Chem. C* **4**, 8704–8710 (2016).
10. Hill, N. A. Where are there so few magnetic ferroelectrics? *J. Phys. Chem. B* **104**, 6694–6709 (2000).
11. Tokura, Y. & Noh, N. D. Unconventional magnetoelectric effects in multiferroic oxides. *Philos. Trans. R. Soc. Lond. Math. Phys. Eng. Sci.* **369**, 3679–3694 (2011).
12. Eerenstein, W., Mathur, N. D. & Scott, J. F. M. Multiferroic and magnetoelectric materials. *Nature* **442**, 759–765 (2006).
13. Kundys, B., Poienar, M. & Simon, C. Effect of coupled ferroelectric and antiferromagnetic interactions on dielectric anomalies in spin-ordered multiferroics. *J. Phys. Condens. Matter* **22**, 445901 (2010).
14. Wang, W. *et al.* Magneto-electric coupling in the paramagnetic state of a metal-organic framework. *Sci. Rep.* **3**, srep02024 (2013).
15. Jain, P. *et al.* Multiferroic behavior associated with an order-disorder hydrogen bonding transition in metal-organic frameworks with the perovskite ABX₃ architecture. *J. Am. Chem. Soc.* **131**, 13625–13627 (2009).
16. Choi, H. *et al.* Ferroelectric porous molecular crystal, $[Mn_3(HCOO)_6](C_2H_5OH)$, exhibiting ferrimagnetic transition. *J. Am. Chem. Soc.* **128**, 15074–15075 (2006).
17. Gómez-Aguirre, L. C. *et al.* Magnetic ordering-induced multiferroic behavior in $[CH_3NH_3][Co(HCOO)_3]$ metal-organic framework. *J. Am. Chem. Soc.* **138**, 1122–1125 (2016).
18. Li, P.-F. *et al.* Unprecedented ferroelectric antiferroelectric paraelectric phase transitions discovered in an organic-inorganic hybrid perovskite. *J. Am. Chem. Soc.* **139**, 8752–8757 (2017).
19. Tian, Y. *et al.* Cross coupling between electric and magnetic orders in a multiferroic metal-organic framework. *Sci. Rep.* **4**, (2014).
20. Frenkel, D.-W. *et al.* A multiferroic perovskite metal-organic framework. *Angew. Chem. Int. Ed.* **50**, 11947–11951 (2011).
21. Rameshkumar, S. Materials science: Emerging routes to multiferroics. *Nature* **461**, 1218–1219 (2009).
22. Li, W. *et al.* Chemically diverse and multifunctional hybrid organic-inorganic perovskites. *Nat. Rev. Mater.* **2**, 201699 (2017).
23. Saparito, B. & Mitzi, D. B. Organic-inorganic perovskites: Structural versatility for functional materials design. *Chem. Rev.* **116**, 4558–4596 (2016).
24. Zhang, W. & Xiong, G.-G. Ferroelectric metal-organic frameworks. *Chem. Rev.* **112**, 1163–1195 (2012).
25. Xu, W.-J. *et al.* A molecular perovskite with switchable coordination bonds for high-temperature multiferroics. *J. Am. Chem. Soc.* **139**, 6369–6375 (2017).
26. Mon, M. *et al.* Postsynthetic approach for the rational design of chiral ferroelectric metal-organic frameworks. *J. Am. Chem. Soc.* **139**, 8098–8101 (2017).
27. Zhang, W.-Y. *et al.* Precise molecular design of high-Tc 3D organic-inorganic perovskite ferroelectric: $[MeHdabco]bI_3$ ($MeHdabco = N$ -Methyl-1,4-diaza-bicyclo[2.2.2]octane). *J. Am. Chem. Soc.* **139**, 10897–10902 (2017).
28. Frenkel, D.-W. *et al.* Diisopropylammonium chloride: A ferroelectric organic salt with a high phase transition temperature and practical utilization of spontaneous polarization. *Adv. Mater.* **23**, 5658–5662 (2011).
29. Frenkel, D.-W. *et al.* Supramolecular bola-like ferroelectric: 4-methoxyanilinium tetraborate-18-crown-6. *J. Am. Chem. Soc.* **133**, 12780–12786 (2011).
30. Frenkel, D.-W. *et al.* 4-methoxyanilinium perchlorate 18-Crown-6: A new ferroelectric with order originating in supramolecular motion. *Phys. Rev. Lett.* **110**, 257601 (2013).
31. Frenkel, D.-W. *et al.* Diisopropylammonium bromide is a high-temperature molecular ferroelectric crystal. *Science* **339**, 425–428 (2013).
32. Zhang, W.-Y., Ye, Q., Frenkel, D.-W. & Xiong, G.-G. Optoelectronic double bistable switches: A biomolecular single crystal and bidirectional triaxial thin film based on imidazole metallochromate. *Adv. Funct. Mater.* **27**, 1603945–1603953 (2017).
33. Jirpichanont, A., Li, F., Shalal, L. A., Iano, N., Prasanna, B. N. & Andre, E. F. Ferroelectricity in the dimethylammonium methylphosphate crystal. *Ferroelectrics* **96**, 313–317 (1989).
34. Japstian, V., Fall, M., Beck, H. & Warhanke, H. Anomalous dielectric behavior of $NH_2(CH_3)_2Al(SO_4)_2 \cdot 6H_2O$ crystals in the ferroelectric phase. *J. Phys. Condens. Matter* **9**, 723 (1997).
35. Vignani, G. *et al.* Local order-disorder behavior in Cr³⁺-doped dimethylammonium methylphosphate heptahydrate (DMAAS) studied by electron paramagnetic resonance. *J. Phys. Condens. Matter* **12**, 4553 (2000).
36. Japstian, V. *et al.* Dielectric and spectral properties of DMAAS ferroelectric crystals doped with chromium. *Phys. Status Solidi A* **201**, 139–147 (2004).
37. Japstian, V. *et al.* Phase transitions and fundamental ferroelectric dispersion in DMAA1-Cr³⁺ crystals. *Acta Phys. Pol. A* **127**, 791–794 (2015).
38. Japstian, V. *et al.* Comparative study of ferroelectric properties of DMAME1-Cr³⁺ (Me = Al, Ga) crystals. *Ferroelectrics* **510**, 80–86 (2017).
39. Shannon, R. D. Revised ionic radii and systematic studies of interatomic distances in halides and chalcogenides. *Acta Crystallogr. A* **32**, 751–767 (1976).

Acknowledgements

This work was partially supported by HYMN, hSTRICSPIN and LABEX research projects. Authors thank Andreas Leithe-Jasper for his careful and critical reading of this manuscript. The technical help of Fabien Chénier is also gratefully acknowledged.